
Ambient Proteins

Training Diffusion Models on Noisy Structures

Anonymous Author(s)

Affiliation

Address

email

Abstract

1 We present *Ambient Protein Diffusion*, a framework for training protein diffusion
2 models that generates structures with unprecedented diversity and quality. State-of-
3 the-art generative models are trained on computationally derived structures from
4 AlphaFold2 (AF), as experimentally determined structures are relatively scarce.
5 The resulting models are therefore limited by the quality of synthetic datasets.
6 Since the accuracy of AF predictions degrades with increasing protein length and
7 complexity, *de novo* generation of long, complex proteins remains challenging.
8 Ambient Protein Diffusion overcomes this problem by treating low-confidence
9 AF structures as corrupted data. Rather than simply filtering out low-quality AF
10 structures, our method adjusts the diffusion objective for each structure based on
11 its corruption level, allowing the model to learn from both high and low quality
12 structures. Empirically, ambient protein diffusion yields major improvements: on
13 proteins with 700 residues, diversity increases from 45% to 85% from the previous
14 state-of-the-art, and designability improves from 70% to 88%.

15 1 Introduction

16 Proteins are the fundamental building block of life. They accelerate chemical reactions by many
17 orders of magnitude, convert sunlight into food, and underpin the myriads of processes within cells
18 and organisms with the level of accuracy and precision required to sustain life [6, 25]. Unlike
19 computational protein engineering—which focuses on improving the developability or function of
20 existing proteins through computationally guided mutations for practical biotechnological applica-
21 tions [17, 31, 20, 32, 8, 29, 16]—*de novo* protein design aims to create entirely new proteins with
22 specified structures and functions, ultimately seeking to discover folds and activities not found in na-
23 ture [10]. Since protein function is largely determined by tertiary and quaternary structure, generative
24 machine learning frameworks for protein design focus on learning the sparse, evolutionarily sampled
25 landscape of protein structures, with the goal of generating novel, functional backbone scaffolds
26 beyond those observed in nature [40, 26, 27, 23, 19, 42, 18, 7, 44, 37].

27 Recent breakthroughs in machine learning-based structure prediction—most notably Al-
28 phaFold2 [24]—have made it possible to infer accurate protein structures directly from se-
29 quence [24, 9, 28]. This progress has enabled the creation of large-scale structural resources such as
30 the AlphaFold Database (AFDB), which contains over 214M predicted structures from UniProtKB
31 sequences [11, 36]. In parallel, high-throughput tools for sequence and structure comparison, such as
32 MMSeqs2 and FoldSeek, have facilitated the curation of large, diverse training datasets from AFDB
33 [5]. Among them, the 2.3M AFDB cluster dataset, has already been shown to improve the capabilities
34 of generative models for protein structure design [27, 19].

35 The quality of a generative model depends on the size and fidelity of its training data. While
36 AlphaFold2 (AF) has enabled large-scale protein structure prediction, its outputs often contain
37 biological or computational inaccuracies [41]. To estimate the reliability of a predicted structure,
38 AlphaFold provides a per-residue confidence score, the predicted Local Distance Difference Test
39 (pLDDT), which is a proxy of local structural accuracy. In practice, researchers frequently filter
40 predicted structures based on average pLDDT scores, training only on high-confidence subsets
41 (typically using a cutoff of $p\text{LDDT} > 80$). Lower pLDDT scores are disproportionately associated
42 with longer and more structurally complex proteins. As a result, filtering based on pLDDT introduces
43 a bias toward smaller, simpler folds, reducing structural diversity in the training set and impairing the
44 model’s ability to generalize to more complex regions of structure space—including longer proteins.
45 Notably, many low-pLDDT structures still contain well-folded domains that are misoriented with
46 respect to each other, as reflected by low predicted alignment error (pAE). These structures can still
47 offer valuable domain-level and coarse-grained information about the structure distribution, which is
48 discarded by overly aggressive filtering.

49 To mitigate these issues, we depart from the standard paradigm of filtering low-confidence structures.
50 Instead, we introduce *Ambient Protein Diffusion* —a framework for training diffusion models
51 that incorporates proteins with noisy or incomplete structures directly into the training process.
52 Ambient Protein Diffusion builds on recent advances in learning generative models from corrupted
53 data [12, 14, 11, 13, 2, 33, 4, 39, 15, 30, 34], which have explored controlled corruption settings such
54 as additive Gaussian noise [12, 14, 1, 15] and masking [13, 2]. Our framework generalizes these
55 techniques to arbitrary, unknown corruption processes, enabling the training of generative models in
56 scientific domains where the corruption mechanism is complex and non-parametric. In our setting, the
57 AlphaFold prediction errors represent such a corruption: they are structured, not explicitly modeled,
58 and vary across protein size and topology. Yet, our method effectively leverages these imperfect
59 samples to significantly advance the capabilities of generative protein models. For example, on
60 proteins with 700 residues, our 16.7M parameter model our method improves diversity from 45% to
61 85% and increases designability from 70% to 88% compared to the previous state-of-the-art, Proteína,
62 a 200M parameter model. Below, we summarize our key contributions:

- 63 • We generalize recent approaches for training generative models on corrupted data to handle
64 arbitrary, non-parametric, and unknown corruption processes, enabling their application to
65 scientific domains.
- 66 • We construct a new training set from the AFDB cluster dataset optimized for geometric
67 diversity, rather than evolutionary similarity, yielding a broader and more representative
68 sampling of structural space for generative modeling.
- 69 • We demonstrate that Ambient Protein Diffusion effectively leverages low-pLDDT AlphaFold
70 predictions, allowing the model to learn from all available samples without distorting the
71 underlying structure distribution.
- 72 • We achieve state-of-the-art results in both diversity and designability for protein generation,
73 improve diversity by 45% and designability by 18% on long proteins (up to 800 residues),
74 and establish the Pareto frontier between these objectives on short proteins (< 256 residues).

75 2 Background and Related Work

76 **De novo Protein Generation.** Most *de novo* protein generation frameworks that operate in structure
77 space follow a three-step pipeline: (1) a generative model samples a three-dimensional backbone
78 structure; (2) an inverse folding model (e.g., ProteinMPNN) proposes amino acid sequences likely
79 to fold into the generated backbone; and (3) these sequences are evaluated by a structure prediction
80 model (e.g., ESMFold) to identify the ones that best recapitulate the target fold.

81 Pioneering methods such as RFDiffusion [40] and Chroma [23] have established strong baselines
82 for backbone generation. More recent advances include Genie [26], which introduces a denoising
83 diffusion model with an $\text{SE}(3)$ -equivariant network that generates proteins as point clouds of reference
84 frames; Genie2 [27], which scales Genie using synthetic AlphaFold structures to improve training
85 data diversity; and Proteína [19], which replaces diffusion with flow matching and scales both model
86 size and dataset scale by orders of magnitude to improve performance on longer and more complex
87 monomeric proteins.

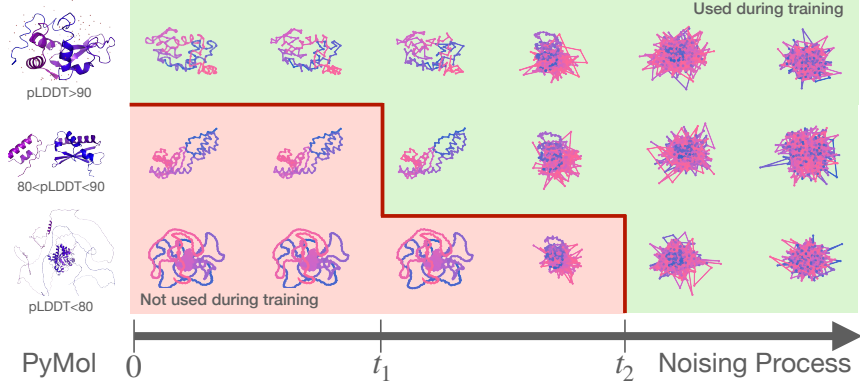


Figure 1: **Overview of Ambient Protein Diffusion on alphafold structures.** Rows 1-3 show the noising process (from left to the right) of three different alphafold proteins based on their average pLDDT (top: high, middle: medium, and bottom:low). These proteins are only used during training at the green diffusion times. At these noise levels, any initial AlphaFold prediction errors in low-pLDDT proteins have effectively been “erased” by the added noise, and the distributions of low- and high-pLDDT proteins have merged.

88 Ambient Protein Diffusion is built using the Genie architecture and makes use of ambient protein
 89 diffusion to achieve state-of-the-art results with substantially shorter training times, much fewer
 90 parameters (16.7M vs 200M), and significantly reduced computational requirements.

91 **Training Datasets.** Recent advances in structure prediction—most notably AlphaFold2 [24] and
 92 ESMFold [28]—have dramatically expanded the available structural data, enabling the prediction
 93 of $\sim 214M$ and $\sim 617M$ monomeric protein structures from UniProtKB (via the AlphaFold Protein
 94 Structure Database) [36] and metagenomic libraries (via the ESM Atlas) [28], respectively. While this
 95 explosion of computational structures presents unprecedented opportunities, it also poses significant
 96 challenges for downstream bioinformatic analysis and model training, particularly due to the scale,
 97 redundancy, and uneven quality of the predicted structures. To address this, prior work applied
 98 MMSeqs2 [22] and FoldSeek [35] to cluster the AlphaFold Database (AFDB), yielding $\sim 2.3M$
 99 clusters designed to capture evolutionary relationships between predicted structures [5]. This AFDB
 100 cluster dataset has since served as the foundational dataset to train several generative protein structure
 101 models [19, 27].

102 In this work, we revisit the FoldSeek pipeline applied AFDB with a different objective: rather than
 103 optimizing for evolutionary insight, we recluster the AFDB cluster dataset with hyperparameters
 104 tuned to maximize geometric diversity. Our goal is to construct a dataset better suited for learning
 105 a generative model of structural space—one that emphasizes structural rather than evolutionary
 106 variation. Starting from the 2.3 million AFDB clusters, we use the cluster representatives with
 107 average $p\text{LDDT} > 70$ ($\sim 1.29M$ structures) and apply our geometric clustering procedure. The
 108 resulting dataset comprises roughly $\sim 292K$ structurally diverse clusters.

109 **Diffusion Models.** The goal in diffusion modeling is to sample from an unknown density p_0 that
 110 we have sample access to. Formally, let $\mathcal{D} = \{x_0^i\}_{i=1}^N$ a dataset of N independent samples, where
 111 $X_0^i \sim p_0$. The unknown distribution p_0 is potentially complex, high-dimensional and multimodal. To
 112 make the sampling problem more tractable, in diffusion modeling we target smoothed densities p_t
 113 defined as the convolution with a Gaussian: $p_t = p_0 * \mathcal{N}(0, \sigma(t)I_d)$ ¹ where $\sigma(t)$ is an increasing
 114 function of t , with $\sigma(0) = 0$. In particular, the object of interest in diffusion modeling is the score-
 115 function of the smoothed densities, defined as $\nabla_{x_t} \log p_t(x_t)$. The latter is connected to the optimal
 116 denoiser (in the l_2 sense) through Tweedie’s Formula: $\nabla \log p_t(x_t) = \frac{\mathbb{E}[X_0 | X_t = x_t] - x_t}{\sigma^2(t)}$.

¹ Alternative formulations of diffusion modeling, such as the Variance Preserving case, are equivalent to this case up to a simple reparametrization. For the ease of analysis, we focus our presentation on corruptions of the form $X_t = X_0 + \sigma_t Z$, $Z \sim \mathcal{N}(0, I_d)$.

117 Given access to $\mathbb{E}[X_0|X_t = x_t]$ one can sample from the distribution p_0 of interest by running a
 118 reverse diffusion process [3]. Hence, the sampling problem becomes equivalent to the problem of
 119 approximating the set of functions $\{\mathbb{E}[X_0|X_t = \cdot]\}_{t=0}^T$. Given a sufficiently rich family of functions
 120 $\{h_\theta : \theta \in \Theta\}$, the conditional expectation at a particular time t can be learned by minimizing the
 121 objective:

$$J(\theta) = \mathbb{E}_{t \in \mathcal{U}[0, T]} \mathbb{E}_{x_0, x_t | t} \left[\|h_\theta(x_t) - x_0\|^2 \right]. \quad (1)$$

122 **Protein Diffusion.** In protein diffusion models that target backbone generation, X_0 captures the 3-D
 123 co-ordinates for each one of the backbone residues of the protein. The length of a protein varies and
 124 the standard practice is to pad each protein to specified length (256 for Genie [26, 27]), with some
 125 special mask indicating the valid positions.

126 **Learning from noisy data.** Recent work has explored the problem of learning diffusion models
 127 from corrupted data. Typically, the corruption process is simple, e.g. it can be additive Gaussian
 128 noise as in [12, 14, 1], or masking as in [1, 2]. Even in works that the corruption process is more
 129 general, the degradation needs to be known and multiple diffusion trainings are required until an
 130 Expectation-Maximization algorithm converges [33, 4]. In this work, we deviate from this setting
 131 as the corruption process is unknown and complex, which may include AlphaFold learning and
 132 hallucination errors, and noise inherent to the structural biology technique used to solve the structure,
 133 etc. We also target a single diffusion training instead of performing multiple EM iterations. The
 134 method is detailed in Section 3.

135 Our work generalizes the techniques developed in [12, 14] for the additive Gaussian noise case.
 136 Particularly, in [14], the authors consider learning from a dataset $\mathcal{D} = \{(x_{t_i}^i, t_i)\}_{i=1}^N$ of samples noised
 137 with additive Gaussian noise of different variances $\{\sigma^2(t_i)\}_{i=1}^N$. Formally, let $X_{t_i} = X_0 + \sigma(t_i)Z$,
 138 where $X_0 \sim p_0, Z \sim \mathcal{N}(0, I_d)$. Each point X_{t_i} contributes to the learning only for $t \geq t_i$, using
 139 the objective:

$$\hat{J}(\theta) = \mathbb{E}_{t \in \mathcal{U}[0, T]} \sum_{x_{t_i} \in \mathcal{D}: t_i > t} \mathbb{E}_{x_t | x_{t_i}, t_i} \left[\|\alpha(t, t_i)h_\theta(x_t, t) + (1 - \alpha(t, t_i))x_t - x_{t_i}\|^2 \right], \quad (2)$$

140 $\alpha(t, t_i) = \frac{\sigma^2(t) - \sigma^2(t_i)}{\sigma^2(t)}$. As the number of samples grows to infinity, Equation 2 also recovers the
 141 conditional expectation $\mathbb{E}[X_0|X_t = x_t]$, but it does so while being able to utilize noisy samples.
 142 This objective recovers the true minimizer because one can prove that the conditional expectation
 143 $\mathbb{E}[X_{t_i}|X_t = x_t]$, lies in the line that connects the current noisy point x_t and the prediction of the
 144 clean image, $\mathbb{E}[X_0|X_t = x_t]$.

145 3 Method

146 Formally, we are given access to samples from the AlphaFold distribution \tilde{p}_0 and aim to learn how
 147 to sample from the true distribution of experimentally solved structures, p_0 , without an explicit
 148 degradation model mapping $p_0 \rightarrow \tilde{p}_0$. In the protein structure setting, it is not appropriate to model
 149 the structural deviations introduced by AlphaFold as additive Gaussian noise. Our key insight is that,
 150 regardless of how \tilde{p}_0 deviates from p_0 , adding noise to both distributions causes them to contract
 151 toward one another. As the noise level increases, the distributions \tilde{p}_t and p_t become progressively
 152 more aligned. This is because it is known that Gaussian noise contracts distribution distances (KL
 153 divergence) in the following sense:

$$D_{KL}(p_t || \tilde{p}_t) \leq D_{KL}(p_{t'} || \tilde{p}_{t'}), \quad \forall t \geq t'. \quad (3)$$

154 In fact, as $t \rightarrow \infty$, we have that: $D_{KL}(p_t || \tilde{p}_t) \rightarrow 0$, as both distributions converge to the same
 155 Gaussian. We now define the concept of merging of two distributions towards the same measure.

156 **Definition 3.1 (ϵ -merged)** *We say that two distributions, p and \tilde{p} are ϵ -merged, if the KL distance
 157 between the two is upper-bounded, by ϵ , i.e., if $D_{KL}(p || \tilde{p}) \leq \epsilon$.*

158 Similarly, we define the merging time of two distributions as the minimal amount of noise we need to
 159 add such that the two distributions become ϵ -merged. Formally,

160 **Definition 3.2 (ϵ -merging time)** Let two distributions p, \tilde{p} . We define their ϵ -merging time as follows:
161 $t_n(p, \tilde{p}, \epsilon) = \inf\{t : D_{\text{KL}}(p * \mathcal{N}(0, \sigma(t)^2 I) || \tilde{p} * \mathcal{N}(0, \sigma(t)^2 I) \leq \epsilon\}$.

162 Assuming we can estimate the ϵ -merging time between two distributions p and \tilde{p} , our key idea is to
163 treat samples from \tilde{p}_t as approximate samples from p_t for all timesteps $t > t_n(p, \tilde{p}, \epsilon)$. This idea is
164 illustrated in Figure 1. The intuition is that once the distributions have sufficiently merged under
165 noise, the residual shift becomes negligible and samples from \tilde{p}_t can be used for learning p_t . This
166 holds because: (i) the learning algorithm may not be sensitive to small distributional discrepancies at
167 high noise levels, and (ii) even if some bias is introduced, the remaining diffusion trajectory for times
168 $t \leq t_n(p, \tilde{p}, \epsilon)$ is robust to small initial distributional mismatch due to its inherent stochasticity.

169 **Sample dependent noise levels.** At a high level, our objective is to determine the ϵ -merging time
170 between the distribution of AlphaFold-predicted structures and that of experimentally resolved
171 proteins. A key challenge arises from the fact that the AlphaFold distribution is highly heterogeneous
172 in structural fidelity—that is, the accuracy with which AlphaFold predicts the true protein structure
173 varies widely across samples. It is well established that short, structurally simple proteins are predicted
174 with higher confidence, while longer and more complex proteins tend to yield lower-confidence
175 predictions. This trend is illustrated in Figure 2B (Left). If we were to assign a single noise level across
176 the entire AlphaFold dataset, we would need to select a relatively high noise level to accommodate the
177 lowest-confidence predictions, particularly from long proteins. This would unnecessarily degrade the
178 training signal for high-confidence structures—regardless of protein length—and limit the model’s
179 ability to learn from clean supervision. To address this, we treat the AlphaFold dataset as a mixture
180 of K sub-distributions, q_1, q_2, \dots, q_K , each representing a distinct confidence regime. We then
181 assign each sub-distribution an appropriate noise level, sufficient to bring it ϵ -close to the distribution
182 of high-confidence structures under the same noise schedule. This formulation allows the model
183 to effectively learn from high-confidence AlphaFold predictions and incorporate low-confidence
184 structures in a controlled manner, mitigating the degradation typically caused by noisy training data.

185 A natural way to decompose the AlphaFold distribution into a mixture of quality-specific sub-
186 distributions is to leverage AlphaFold’s self-reported confidence metric—the average predicted
187 Local Distance Difference Test (pLDDT) score—as a proxy for predicted structural fidelity. In
188 particular, given a dataset $\mathcal{D} = \{(x_0^{(i)}, \text{pLDDT}^{(i)})\}_{i=1}^N$, we consider K distributions (where K is
189 a hyperparameter to be chosen) with empirical observations for the j -th distribution being all the
190 samples $\{(x_0^{(i)}, \text{pLDDT}^{(i)}) : c_{\min}^{(j)} \leq \text{pLDDT}^{(i)} \leq c_{\max}^{(j)}\}$, for some hyperparameters $c_{\min}^{(j)}, c_{\max}^{(j)}$.

191 **Choice of sub-distribution boundaries.** In this work, we adopt a deliberately simple and conservative
192 strategy by partitioning the AlphaFold dataset into three discrete quality regimes based on the average
193 pLDDT score: high-quality proteins ($\text{pLDDT} > 90$), medium-quality proteins (pLDDT in $[80, 90]$)
194 and low-quality proteins (pLDDT in $[70, 80]$). We acknowledge that this discretization is coarse and
195 that more principled alternatives may yield further improvements—for instance, by optimizing the bin
196 boundaries or learning a continuous mapping from pLDDT to diffusion time. Despite the simplicity
197 of our choices, our experimental results demonstrate that even a naive quality-aware decomposition
198 can lead to important gains in performance across both short and long proteins. There are two sources
199 of benefit over filtering methods: 1) low-quality data (previously discarded) give diversity and 2) the
200 distinction we do between medium-quality and high-quality data increases designability.

201 **Ambient Protein Diffusion Algorithm.** Our algorithm takes as input a dataset of protein structures
202 together with their average pLDDT score, $\mathcal{D} = \{(x_0^{(i)}, \text{pLDDT}^{(i)})\}_{i=1}^N$, a diffusion schedule, $\sigma(t)$,
203 and a mapping function $f : [0, 100] \mapsto \mathbb{R}^+$ that translates the average pLDDT value of a protein to
204 its estimated ϵ -merging time.

205 **Annotation stage.** The first step of the algorithm replaces each protein in the dataset with a noisy
206 version of itself, where the noise level is determined by mapping function f . After this transformation,
207 each protein can be treated as a sample from the target distribution convolved with a Gaussian at
208 its assigned noise level. Importantly, this corruption step is only performed once during dataset
209 preprocessing.

210 **Loss function.** After the annotation stage, we need to solve a training problem where we have data
211 corrupted at different noise levels with additive Gaussian noise, as in [12, 14]. Hence, we can use the
212 objective of Equation 2

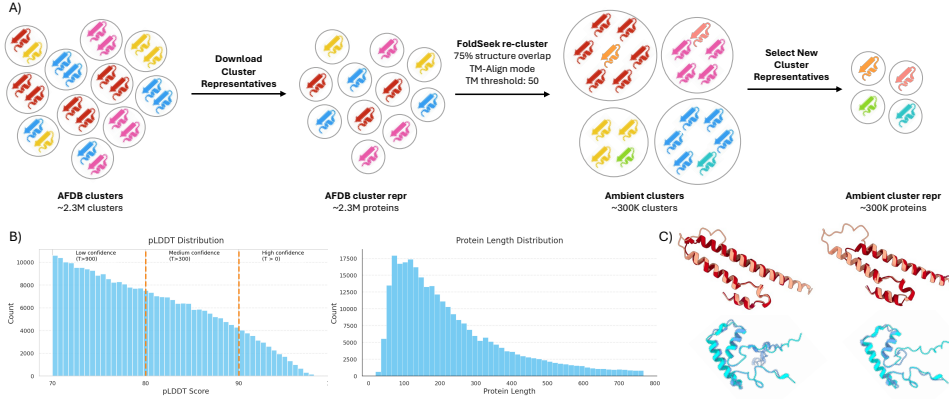


Figure 2: Reclustering the AFDB cluster dataset for generative protein modeling. (A) Starting from the 2.3M clusters in the AFDB, we cluster the representatives with FoldSeek with alignment-type set to TM-Align, TM threshold set to 0.5, and coverage set to 0.75. This results in 300K cluster ($p\text{LDDT} > 70$) from which we keep the representatives for training. (B) $p\text{LDDT}$ and protein length statistics for our new training set. (C) Example of two protein clusters where two cluster members (red and blue) are superimposed with their cluster representative (beige and cyan).

213 Instead of directly applying the loss, we first need to rescale each time t to account for the vanishing
 214 gradient effect that is due to the multiplicative factor $a(t)$. Specifically, we need to rescale the loss at
 215 time t with: $w(t) = \frac{1}{a^2(t)} = \frac{\sigma^4(t)}{(\sigma^2(t) - \sigma^2(t_0))^2}$. We underline that this rescaling was not mentioned in
 216 the original paper of Daras et al. [14] [12], for training with noisy data. Yet, we find this rescaling
 217 critical for the success of our method. We hypothesize that the authors of [12] [14] did not encounter
 218 this issue because there were at most two noise levels considered, while in AF predicted protein
 219 structures there is a whole spectrum of assigned noise levels based on the predicted quality (measured
 220 by average $p\text{LDDT}$) of a protein structure. We provide further details about the loss implementation
 221 in the supplement and pseudocode for our Algorithm in the Appendix.

222 **Uniform Protein Sampling in terms of diffusion times.** To perform a training update for a diffusion
 223 model, we typically sample a point from the training distribution and then we uniformly sample the
 224 noise level t . However, since in our case we are dealing with noisy data, not all times t are allowed
 225 for a given protein, i.e. a protein with $p\text{LDDT}^{(i)}$ is only used for times $t \geq f(p\text{LDDT}^{(i)})$. To
 226 avoid spending most of the training updates on very noisy proteins, we opt for sampling first the
 227 diffusion time and then select from the eligible proteins that can be used in that diffusion time. This
 228 strategy ensures balanced coverage across the diffusion trajectory—from low to high noise—while
 229 still leveraging the diversity of low-confidence structures ($p\text{LDDT} < 80$) in our training dataset.

230 **Reclustering AFDB clusters for generative modeling applications.** The AFDB cluster dataset [5]
 231 has been used to train several generative protein models [27] [19]. However, the original intent behind
 232 the clustering was to study structure evolution across AFDB. Thus, the hyperparameters were chosen
 233 to obtain clusters of homologous structures, and the authors report that 97.4% of pairwise comparisons
 234 within clusters are conserved at the H-group (Homology) level of the ECOD hierarchical domain
 235 classification (median TM-score 0.71). While these FoldSeek hyperparameters are well-suited for
 236 evolutionary analysis of AFDB, we found that the AFDB cluster dataset has a significant degree of
 237 structural duplication and near-duplication between clusters that are more distantly evolutionarily
 238 related (see Figure 2C). This structural redundancy leads to an imbalanced training set, where
 239 structural motifs from the larger protein superfamilies are overrepresented.

240 Given this finding, we hypothesized that the datasets for generative modeling of protein struc-
 241 tures—particularly for backbone-based models—benefit more from clusters defined purely by
 242 geometric similarity. To address this, we constructed a new clustering dataset derived from the AFDB
 243 cluster representatives, with an exclusive focus on structural topology. Specifically, these are the
 244 changes we made to the FoldSeek hyperparameters: switched the alignment-type from 3Di+AA to
 245 TM-Align to improve fidelity, used a TM-score threshold of 0.5, and relaxed the alignment coverage

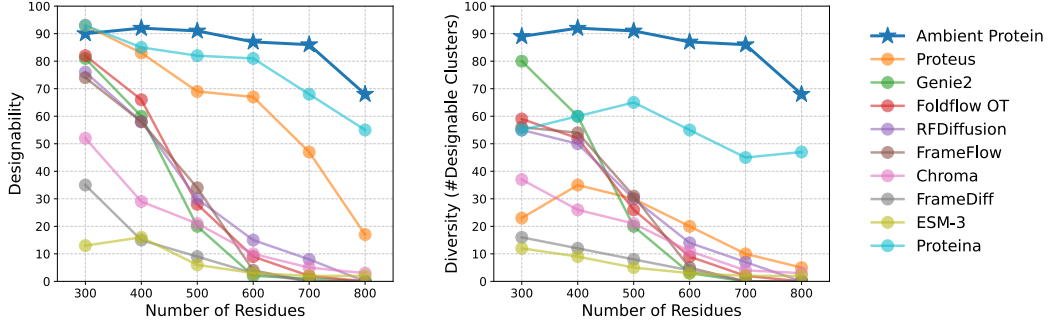


Figure 3: **Long protein generation performance.** We fine-tune Ambient Protein Diffusion on proteins up to 768 residues and sample sequences ranging from 300 to 800 residues. Ambient Protein Diffusion generates diverse and designable structures across this length range with consistent performance.

from 0.9 to 0.75. We relaxed the alignment coverage to improve clustering of AlphaFolded proteins with extended, unfolded N- or C-terminal regions (i.e., noodle tails) (Figure 2C). This approach produced a more balanced dataset that samples structural folds more uniformly, independent of their evolutionary relationships. Ablations showing the contribution of this reclustering versus our ambient training approach are given in Figure 4.

4 Experimental Results

We build on the Genie2 codebase [27]. Our model architecture follows the Genie2 architecture except that it is scaled larger, using 8 triangle layers as opposed to 5. We follow Genie2’s schedule for inference time sampling and diffuse for 1000 timesteps.

We train Ambient Protein Diffusion in 3 stages with increasingly longer proteins. In first stage, we train on proteins from 50 to 256 residues for 200 epochs on our ambient clusters dataset using the representatives ($\sim 196,000$ proteins). Since we increased the batch size to 384 items, we adopted a learning rate schedule to improve convergence [21]. We train with the AdamW optimizer with a maximal learning rate of 1.0×10^{-4} . During the second and third stage, we include additional cluster representatives of at most 512 and 712 residues, which scales our dataset to $\sim 269,000$ and $\sim 291,000$ proteins respectively. Training is performed on 48 GH200 GPUs and runs in 18, 48, and 48 hours for each stage respectively. More hyperparameters and details about our evaluation metrics can be found in the supplement. We underline that the computational cost of training our model, while significant, is still relatively low compared to the Proteína’s estimated 14 days training on 128 A100 GPUs. This is due to the decreased size of our model (< 17M vs 200M) and training set ($\sim 290K$ vs $\sim 780K$). We further note that our goal is to develop models that perform well across a range of tasks, including long-protein generation, motif scaffolding, and more. To this end, we train only two models for the purposes of this paper: one model optimized for long-protein generation (Figure 3) and another optimized for short-protein generation (Figure 4).

Comparisons on unconditional generation of longer proteins.

In Figure 3, we compare Ambient Protein Diffusion performance on generating backbone for proteins with length ranging from 300 to 800 residues. To directly compare with Proteína on long-protein generation, we adopt its three-stage training and evaluation protocol. During training, the maximum sequence length is capped at 768 residues. For evaluation, we sample 100 protein backbones at each target length and evaluate them using the designability and diversity metrics. Since Ambient Protein Diffusion builds on Genie2, we use the same sampling procedure—running 1000 diffusion steps with a noise scale of $\gamma = 0.6$.

Ambient Protein Diffusion achieves designability and diversity scores exceeding 90% for proteins between 300 and 500 residues, and maintains scores above 85% for lengths up to 700 residues. For 800-residue proteins, both metrics decline to 68%. Compared to Proteína, Ambient Protein Diffusion outperforms by 26% in designability and 91% in diversity at length 700, and by 25% and 44%, respectively, at length 800. At every protein length, Ambient Protein Diffusion’s diversity is equal to

283 its designability, indicating that every designable protein is unique. This is not the case for Proteína,
284 where diversity scores consistently fall below designability, regardless of protein length.

285 Taken together, these results demonstrate the impact of ambient diffusion on backbone-based generative
286 models and highlight the strength of Genie2’s equivariant architecture. Our 17M parameter model
287 trained on approximately 290K AlphaFold structures significantly outperforms a 200M-parameter
288 transformer model trained on roughly 780K proteins. Our results show that smaller, more efficient
289 models can surpass larger transformer baselines in both structural diversity and designability.

Comparisons on unconditional generation of shorter proteins. In this experiment, we evaluate the model on the unconditional generation of shorter proteins in Figure 4. The Ambient Protein Diffusion model used in this experiment was trained on a dataset filtered with a TM-Align threshold of 0.4 (as opposed to 0.5), resulting in a training set of approximately 90K cluster representative proteins.

Following the Genie2 protocol, we generate 5 structures for each sequence length from 50 to 256 residues, yielding a total of 1,035 structures. The generated structures are evaluated for both designability and diversity. In line with prior work, we sweep the noise scale γ to explore the tradeoff between designability and diversity. Ambient Protein Diffusion outperforms previous methods on both metrics, establishing a new Pareto frontier that achieves superior performance compared to all existing models, including Proteina. While it is well known that protein pairs with TM-scores above 0.5 typically share the same fold, and those below 0.5 generally do not, we find that the trade-off between designability and diversity is sensitive to the underlying structural heterogeneity of the dataset. Notably, clustering with a TM-align threshold of 0.4, which corresponds to less than a 1% chance of shared global topology, slightly outperforms the 0.5 threshold, which reflects a $\sim 38\%$ probability of topological similarity [43].

314 Ablating the Significance of Ambi-
315 ent Diffusion. We validate the effec-
316 tiveness of Ambient Diffusion in Fig-
317 ure 5. For our ablation, we perform
318 the identical three stages of training
319 on a model variant that performs stan-
320 dard diffusion training as opposed to
321 Ambient Diffusion. The Genie2 base-
322 line is taken from the Proteína paper.
323 We find that while our two models per-
324 form similarly on proteins of 300 residu-
325 diminishes much more significantly wi-
326 of designable clusters drops from 68%

Comparisons on Motif Scaffolding. We additionally compare our method to prior work on motif scaffolding in Figure 6, with full results provided in the supplement. Our evaluation follows the Genie2 benchmark, which comprises 24 single-motif and 6 multi-motif design tasks [27, 40]. For each task, we generate 1,000 scaffold samples using a noise scale of $\gamma = 0.45$. A design is considered successful if it (1) satisfies Genie2’s motif designability criteria and (2) preserves the motif with an RMSD below 1 Å. Among successful designs, a scaffold is unique if its TM-score is at most 0.6 when compared to any other successful scaffold. A task is considered solved if at least one successful scaffold is generated.

With $\gamma = 0.45$, Ambient Protein Diffusion generates 1,923 unique successful scaffolds for single-motif tasks, a significant improvement over Genie2's 1,445 [27] and performs comparably to Proteína's 2,094 [19]. Notably, all methods solve a similar number of motifs – RFDiffusion solves 22 of

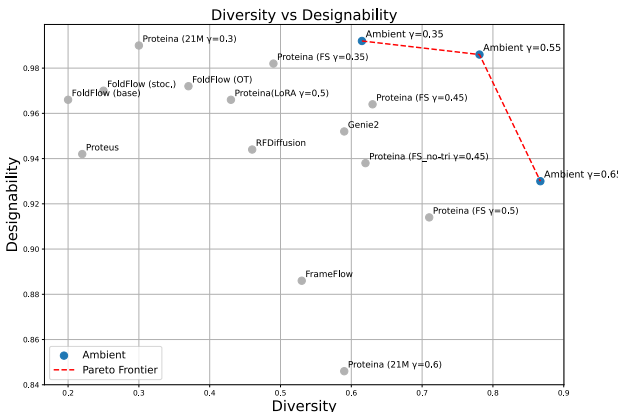


Figure 4: **Designability - diversity trade-off for short protein generation** (up to 256 residues). Ambient dominates completely the Pareto frontier between designability and diversity, while using a $12.88 \times$ smaller model. We further do so without using any higher-order sampler or (auto-) guidance method.

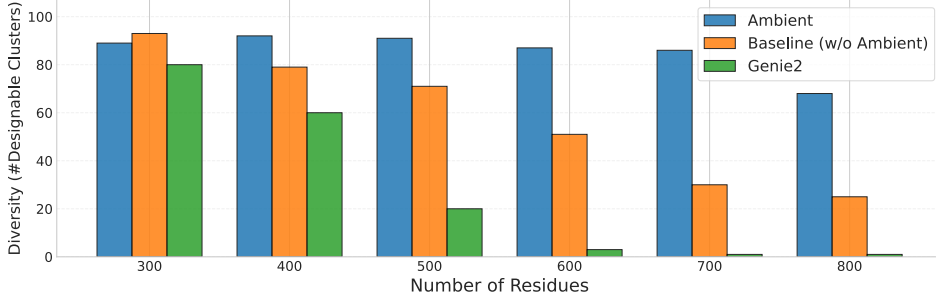


Figure 5: Effect of ambient diffusion on long protein generation. We sample protein sequences ranging from 300 to 800 residues. The baseline model (without Ambient Diffusion) shares the same architecture and training dataset, differing only in the diffusion loss and sampling procedure. At a sequence length of 300, the baseline yields four additional designable clusters. However, Ambient Protein Diffusion consistently outperforms both the baseline and Genie2, with increasingly significant improvements as sequence length grows.

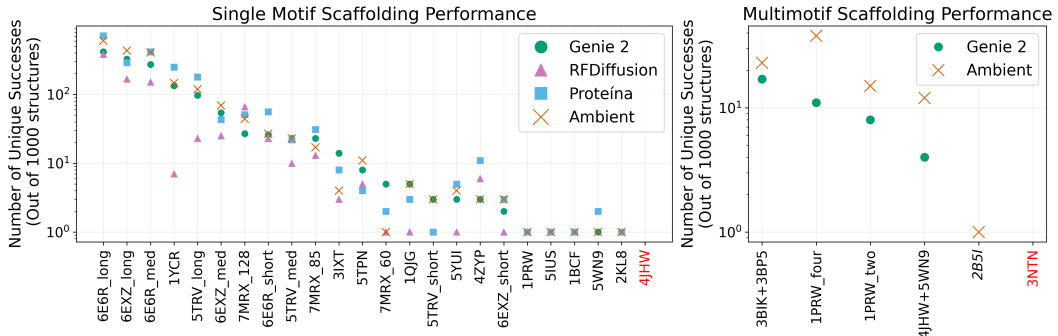


Figure 6: Performance on Motif Scaffolding Tasks. We compare Ambient Protein Diffusion to state-of-the-art models for motif scaffolding. The graphs show the number of unique successful scaffolds generated for each single- and multi-motif task. No model produced successful scaffolds for **4JHW** and **3NTN**. Only Ambient Protein Diffusion produced a valid solution for multi-motif scaffolding of **2B5I**.

338 the 24 tasks, while Ambient Protein Diffusion, Genie2, and Proteína each solve the same 23 tasks. For
 339 multi-motif scaffolding, Ambient Protein Diffusion generates 89 unique successful structures across
 340 5 of the 6 benchmark problems, outperforming Genie2, which produces 40 and solves 4. Ambient
 341 Protein Diffusion performs particularly well on the 1PRW_four motif (38 vs. 11 successful structures)
 342 in which a scaffold is generated surrounding a calcium binding motif [38]. Overall, Ambient Protein
 343 Diffusion outperforms existing methods such as Genie2 and RFDiffusion on single-motif tasks and
 344 matches the performance of a Proteína model optimized specifically for motif-scaffolding.

345 5 Conclusion

346 We introduced *Ambient Protein Diffusion*, a diffusion-based model for protein structure generation
 347 that leverages low-confidence AlphaFold structures as a source of noisy training data. Ambient
 348 Protein Diffusion enables the generation of long protein structures with unprecedented levels of
 349 designability and diversity. Diversity increases as it can use low-confidence AlphaFold structures
 350 that are typically discarded and designability increases as we separate the pristine quality protein
 351 structures from the medium quality AlphaFold predictions. Ambient Protein Diffusion represents a
 352 foundational step toward robust de novo protein design at more natural, biologically relevant lengths.
 353 Despite progress, Ambient Protein Diffusion still favors generating alpha-helical structures and
 354 developing techniques that address this bias is a crucial direction for future work.

355 **References**

356 [1] Asad Aali, Marius Arvinte, Sidharth Kumar, and Jonathan I Tamir. Solving inverse problems
357 with score-based generative priors learned from noisy data. *arXiv preprint arXiv:2305.01166*,
358 2023.

359 [2] Asad Aali, Giannis Daras, Brett Levac, Sidharth Kumar, Alex Dimakis, and Jon Tamir. Ambient
360 diffusion posterior sampling: Solving inverse problems with diffusion models trained on
361 corrupted data. In *The Thirteenth International Conference on Learning Representations*, 2025.
362 URL <https://openreview.net/forum?id=qeXcMutEZY>

363 [3] Brian D.O. Anderson. Reverse-time diffusion equation models. *Stochastic Processes and their*
364 *Applications*, 12(3):313–326, 1982.

365 [4] Weimin Bai, Yifei Wang, Wenzheng Chen, and He Sun. An expectation-maximization al-
366 gorithm for training clean diffusion models from corrupted observations. *arXiv preprint*
367 *arXiv:2407.01014*, 2024.

368 [5] Inigo Barrio-Hernandez, Jingi Yeo, Jürgen Jänes, Milot Mirdita, Cameron LM Gilchrist, Tanita
369 Wein, Mihaly Varadi, Sameer Velankar, Pedro Beltrao, and Martin Steinegger. Clustering
370 predicted structures at the scale of the known protein universe. *Nature*, 622(7983):637–645,
371 2023.

372 [6] Jeremy M Berg, John L Tymoczko, and Lubert Stryer. *Biochemistry (loose-leaf)*. Macmillan,
373 2007.

374 [7] Avishek Joey Bose, Tara Akhoud-Sadegh, Guillaume Huguet, Kilian Fatras, Jarrid Rector-
375 Brooks, Cheng-Hao Liu, Andrei Cristian Nica, Maksym Korablyov, Michael Bronstein, and
376 Alexander Tong. Se (3)-stochastic flow matching for protein backbone generation. *arXiv*
377 *preprint arXiv:2310.02391*, 2023.

378 [8] Jose M Carceller, Bhumika Jayee, Claire G Page, Daniel G Oblinsky, Gustavo Mondragón-
379 Solórzano, Nithin Chintala, Jingzhe Cao, Zayed Alassad, Zheyu Zhang, Nathaniel White, et al.
380 Engineering a photoenzyme to use red light. *Chem*, 11(2), 2025.

381 [9] Xinshi Chen, Yuxuan Zhang, Chan Lu, Wenzhi Ma, Jiaqi Guan, Chengyue Gong, Jincai Yang,
382 Hanyu Zhang, Ke Zhang, Shenghao Wu, Kuangqi Zhou, Yanping Yang, Zhenyu Liu, Lan Wang,
383 Bo Shi, Shaochen Shi, and Wenzhi Xiao. Protex - advancing structure prediction through a
384 comprehensive alphafold3 reproduction. *bioRxiv*, 2025. doi: 10.1101/2025.01.08.631967.

385 [10] Alexander E Chu, Tianyu Lu, and Po-Ssu Huang. Sparks of function by de novo protein design.
386 *Nature biotechnology*, 42(2):203–215, 2024.

387 [11] UniProt Consortium. Uniprot: a hub for protein information. *Nucleic acids research*, 43(D1):
388 D204–D212, 2015.

389 [12] Giannis Daras, Yuval Dagan, Alexandros G Dimakis, and Constantinos Daskalakis. Consistent
390 diffusion models: Mitigating sampling drift by learning to be consistent. *arXiv preprint*
391 *arXiv:2302.09057*, 2023.

392 [13] Giannis Daras, Kulin Shah, Yuval Dagan, Aravind Gollakota, Alex Dimakis, and Adam Klivans.
393 Ambient diffusion: Learning clean distributions from corrupted data. In *Thirty-seventh Con-
394 ference on Neural Information Processing Systems*, 2023. URL [https://openreview.net/for-
395 um?id=wBJBLy9kBY](https://openreview.net/for-
395 um?id=wBJBLy9kBY)

396 [14] Giannis Daras, Alexandros G Dimakis, and Constantinos Daskalakis. Consistent diffusion
397 meets tweedie: Training exact ambient diffusion models with noisy data. *arXiv preprint*
398 *arXiv:2404.10177*, 2024.

399 [15] Giannis Daras, Yeshwanth Cherapanamjeri, and Constantinos Costis Daskalakis. How much is
400 a noisy image worth? data scaling laws for ambient diffusion. In *The Thirteenth International*
401 *Conference on Learning Representations*, 2025. URL [https://openreview.net/forum?
402 id=qZwtPEw2qN](https://openreview.net/forum?
402 id=qZwtPEw2qN)

403 [16] Daniel J Diaz, Anastasiya V Kulikova, Andrew D Ellington, and Claus O Wilke. Using machine
404 learning to predict the effects and consequences of mutations in proteins. *Current opinion in*
405 *structural biology*, 78:102518, 2023.

406 [17] Daniel J Diaz, Chengyue Gong, Jeffrey Ouyang-Zhang, James M Loy, Jordan Wells, David
407 Yang, Andrew D Ellington, Alexandros G Dimakis, and Adam R Klivans. Stability oracle:
408 a structure-based graph-transformer framework for identifying stabilizing mutations. *Nature*
409 *Communications*, 15(1):6170, 2024.

410 [18] Cong Fu, Keqiang Yan, Limei Wang, Wing Yee Au, Michael Curtis McThrow, Tao Komikado,
411 Koji Maruhashi, Kanji Uchino, Xiaoning Qian, and Shuiwang Ji. A latent diffusion model for
412 protein structure generation. In *Learning on Graphs Conference*, pages 29–1. PMLR, 2024.

413 [19] Tomas Geffner, Kieran Didi, Zuobai Zhang, Danny Reidenbach, Zhonglin Cao, Jason Yim,
414 Mario Geiger, Christian Dallago, Emine Kucukbenli, Arash Vahdat, et al. Proteina: Scaling
415 flow-based protein structure generative models. *arXiv preprint arXiv:2503.00710*, 2025.

416 [20] Chengyue Gong, Adam Klivans, James Madigan Loy, Tianlong Chen, Daniel Jesus Diaz, et al.
417 Evolution-inspired loss functions for protein representation learning. In *Forty-first International*
418 *Conference on Machine Learning*, 2024.

419 [21] Priya Goyal, Piotr Dollár, Ross Girshick, Pieter Noordhuis, Lukasz Wesolowski, Aapo Kyrola,
420 Andrew Tulloch, Yangqing Jia, and Kaiming He. Accurate, large minibatch sgd: Training
421 imangenet in 1 hour. *arXiv preprint arXiv:1706.02677*, 2017.

422 [22] Maria Hauser, Martin Steinegger, and Johannes Söding. Mmseqs software suite for fast and
423 deep clustering and searching of large protein sequence sets. *Bioinformatics*, 32(9):1323–1330,
424 2016.

425 [23] John B Ingraham, Max Baranov, Zak Costello, Karl W Barber, Wujie Wang, Ahmed Ismail,
426 Vincent Frappier, Dana M Lord, Christopher Ng-Thow-Hing, Erik R Van Vlack, et al. Illumi-
427 nating protein space with a programmable generative model. *Nature*, 623(7989):1070–1078,
428 2023.

429 [24] John Jumper, Richard Evans, Alexander Pritzel, Tim Green, Michael Figurnov, Olaf Ron-
430 neberger, Kathryn Tunyasuvunakool, Russ Bates, Augustin Žídek, Anna Potapenko, et al. Highly
431 accurate protein structure prediction with alphafold. *nature*, 596(7873):583–589, 2021.

432 [25] Albert L Lehninger, David L Nelson, and Michael M Cox. *Lehninger principles of biochemistry*.
433 Macmillan, 2005.

434 [26] Yeqing Lin and Mohammed AlQuraishi. Generating novel, designable, and diverse protein
435 structures by equivariantly diffusing oriented residue clouds. *arXiv preprint arXiv:2301.12485*,
436 2023.

437 [27] Yeqing Lin, Minji Lee, Zhao Zhang, and Mohammed AlQuraishi. Out of many, one: Designing
438 and scaffolding proteins at the scale of the structural universe with genie 2. *arXiv preprint*
439 *arXiv:2405.15489*, 2024.

440 [28] Zeming Lin, Halil Akin, Roshan Rao, Brian Hie, Zhongkai Zhu, Wenting Lu, Nikita Smetanin,
441 Robert Verkuil, Ori Kabeli, Yaniv Shmueli, et al. Evolutionary-scale prediction of atomic-level
442 protein structure with a language model. *Science*, 379(6637):1123–1130, 2023.

443 [29] Yi Liu, Sophie G Bender, Damien Sorigue, Daniel J Diaz, Andrew D Ellington, Greg Mann,
444 Simon Allmendinger, and Todd K Hyster. Asymmetric synthesis of α -chloroamides via
445 photoenzymatic hydroalkylation of olefins. *Journal of the American Chemical Society*, 146(11):
446 7191–7197, 2024.

447 [30] Haoye Lu, Qifan Wu, and Yaoliang Yu. SFBD: A method for training diffusion models with
448 noisy data. In *Frontiers in Probabilistic Inference: Learning meets Sampling*, 2025. URL
449 <https://openreview.net/forum?id=6HN14zuHRb>.

450 [31] Jeffrey Ouyang-Zhang, Daniel Diaz, Adam Klivans, and Philipp Krähenbühl. Predicting a
451 protein’s stability under a million mutations. *Advances in Neural Information Processing
452 Systems*, 36:76229–76247, 2023.

453 [32] Jeffrey Ouyang-Zhang, Chengyue Gong, Yue Zhao, Philipp Krähenbühl, Adam R Klivans, and
454 Daniel J Diaz. Distilling structural representations into protein sequence models. *bioRxiv*, pages
455 2024–11, 2024.

456 [33] François Rozet, Gérôme Andry, François Lanusse, and Gilles Louppe. Learning diffusion priors
457 from observations by expectation maximization. *arXiv preprint arXiv:2405.13712*, 2024.

458 [34] Kulin Shah, Alkis Kalavasis, Adam R. Klivans, and Giannis Daras. Does generation require
459 memorization? creative diffusion models using ambient diffusion, 2025.

460 [35] Michel van Kempen, Stephanie S Kim, Charlotte Tumescheit, Milot Mirdita, Cameron LM
461 Gilchrist, Johannes Söding, and Martin Steinegger. Foldseek: fast and accurate protein structure
462 search. *Biorxiv*, pages 2022–02, 2022.

463 [36] Mihaly Varadi, Stephen Anyango, Mandar Deshpande, Sreenath Nair, Cindy Natassia, Galabina
464 Yordanova, David Yuan, Oana Stroe, Gemma Wood, Agata Laydon, et al. AlphaFold protein
465 structure database: massively expanding the structural coverage of protein-sequence space with
466 high-accuracy models. *Nucleic acids research*, 50(D1):D439–D444, 2022.

467 [37] Chentong Wang, Yannan Qu, Zhangzhi Peng, Yukai Wang, Hongli Zhu, Dachuan Chen, and
468 Longxing Cao. Proteus: exploring protein structure generation for enhanced designability and
469 efficiency. *bioRxiv*, pages 2024–02, 2024.

470 [38] Jue Wang, Sidney Lisanza, David Juergens, Doug Tischer, Joseph L Watson, Karla M Castro,
471 Robert Ragotte, Amijai Saragovi, Lukas F Milles, Minkyung Baek, et al. Scaffolding protein
472 functional sites using deep learning. *Science*, 377(6604):387–394, 2022.

473 [39] Yifei Wang, Weimin Bai, Weijian Luo, Wenzheng Chen, and He Sun. Integrating amortized
474 inference with diffusion models for learning clean distribution from corrupted images. *arXiv
475 preprint arXiv:2407.11162*, 2024.

476 [40] Joseph L Watson, David Juergens, Nathaniel R Bennett, Brian L Trippe, Jason Yim, Helen E
477 Eisenach, Woody Ahern, Andrew J Borst, Robert J Ragotte, Lukas F Milles, et al. De novo
478 design of protein structure and function with rfdiffusion. *Nature*, 620(7976):1089–1100, 2023.

479 [41] Carter J Wilson, Wing-Yiu Choy, and Mikko Karttunen. AlphaFold2: a role for disordered
480 protein/region prediction? *International Journal of Molecular Sciences*, 23(9):4591, 2022.

481 [42] Kevin E Wu, Kevin K Yang, Rianne van den Berg, Sarah Alamdari, James Y Zou, Alex X Lu,
482 and Ava P Amini. Protein structure generation via folding diffusion. *Nature communications*,
483 15(1):1059, 2024.

484 [43] Jinrui Xu and Yang Zhang. How significant is a protein structure similarity with tm-score= 0.5?
485 *Bioinformatics*, 26(7):889–895, 2010.

486 [44] Jason Yim, Andrew Campbell, Andrew YK Foong, Michael Gastegger, José Jiménez-Luna,
487 Sarah Lewis, Victor Garcia Satorras, Bastiaan S Veeling, Regina Barzilay, Tommi Jaakkola, et al.
488 Fast protein backbone generation with se (3) flow matching. *arXiv preprint arXiv:2310.05297*,
489 2023.

490 **NeurIPS Paper Checklist**

491 **1. Claims**

492 Question: Do the main claims made in the abstract and introduction accurately reflect the
493 paper's contributions and scope?

494 Answer: **[Yes]**

495 Justification: The claims made in the abstract and introduction are validated in the experi-
496 mental results

497 Guidelines:

- 498 • The answer NA means that the abstract and introduction do not include the claims
499 made in the paper.
- 500 • The abstract and/or introduction should clearly state the claims made, including the
501 contributions made in the paper and important assumptions and limitations. A No or
502 NA answer to this question will not be perceived well by the reviewers.
- 503 • The claims made should match theoretical and experimental results, and reflect how
504 much the results can be expected to generalize to other settings.
- 505 • It is fine to include aspirational goals as motivation as long as it is clear that these goals
506 are not attained by the paper.

507 **2. Limitations**

508 Question: Does the paper discuss the limitations of the work performed by the authors?

509 Answer: **[Yes]**

510 Justification: See conclusion section.

511 Guidelines:

- 512 • The answer NA means that the paper has no limitation while the answer No means that
513 the paper has limitations, but those are not discussed in the paper.
- 514 • The authors are encouraged to create a separate "Limitations" section in their paper.
- 515 • The paper should point out any strong assumptions and how robust the results are to
516 violations of these assumptions (e.g., independence assumptions, noiseless settings,
517 model well-specification, asymptotic approximations only holding locally). The authors
518 should reflect on how these assumptions might be violated in practice and what the
519 implications would be.
- 520 • The authors should reflect on the scope of the claims made, e.g., if the approach was
521 only tested on a few datasets or with a few runs. In general, empirical results often
522 depend on implicit assumptions, which should be articulated.
- 523 • The authors should reflect on the factors that influence the performance of the approach.
524 For example, a facial recognition algorithm may perform poorly when image resolution
525 is low or images are taken in low lighting. Or a speech-to-text system might not be
526 used reliably to provide closed captions for online lectures because it fails to handle
527 technical jargon.
- 528 • The authors should discuss the computational efficiency of the proposed algorithms
529 and how they scale with dataset size.
- 530 • If applicable, the authors should discuss possible limitations of their approach to
531 address problems of privacy and fairness.
- 532 • While the authors might fear that complete honesty about limitations might be used by
533 reviewers as grounds for rejection, a worse outcome might be that reviewers discover
534 limitations that aren't acknowledged in the paper. The authors should use their best
535 judgment and recognize that individual actions in favor of transparency play an impor-
536 tant role in developing norms that preserve the integrity of the community. Reviewers
537 will be specifically instructed to not penalize honesty concerning limitations.

538 **3. Theory assumptions and proofs**

539 Question: For each theoretical result, does the paper provide the full set of assumptions and
540 a complete (and correct) proof?

541 Answer: **[NA]**

542 Justification:

543 Guidelines:

- 544 • The answer NA means that the paper does not include theoretical results.
- 545 • All the theorems, formulas, and proofs in the paper should be numbered and cross-
546 referenced.
- 547 • All assumptions should be clearly stated or referenced in the statement of any theorems.
- 548 • The proofs can either appear in the main paper or the supplemental material, but if
549 they appear in the supplemental material, the authors are encouraged to provide a short
550 proof sketch to provide intuition.
- 551 • Inversely, any informal proof provided in the core of the paper should be complemented
552 by formal proofs provided in appendix or supplemental material.
- 553 • Theorems and Lemmas that the proof relies upon should be properly referenced.

554 **4. Experimental result reproducibility**

555 Question: Does the paper fully disclose all the information needed to reproduce the main ex-
556 perimental results of the paper to the extent that it affects the main claims and/or conclusions
557 of the paper (regardless of whether the code and data are provided or not)?

558 Answer: [Yes]

559 Justification: We provide thorough implementation details in the paper and supplement.

560 Guidelines:

- 561 • The answer NA means that the paper does not include experiments.
- 562 • If the paper includes experiments, a No answer to this question will not be perceived
563 well by the reviewers: Making the paper reproducible is important, regardless of
564 whether the code and data are provided or not.
- 565 • If the contribution is a dataset and/or model, the authors should describe the steps taken
566 to make their results reproducible or verifiable.
- 567 • Depending on the contribution, reproducibility can be accomplished in various ways.
568 For example, if the contribution is a novel architecture, describing the architecture fully
569 might suffice, or if the contribution is a specific model and empirical evaluation, it may
570 be necessary to either make it possible for others to replicate the model with the same
571 dataset, or provide access to the model. In general, releasing code and data is often
572 one good way to accomplish this, but reproducibility can also be provided via detailed
573 instructions for how to replicate the results, access to a hosted model (e.g., in the case
574 of a large language model), releasing of a model checkpoint, or other means that are
575 appropriate to the research performed.
- 576 • While NeurIPS does not require releasing code, the conference does require all submis-
577 sions to provide some reasonable avenue for reproducibility, which may depend on the
578 nature of the contribution. For example
 - 579 (a) If the contribution is primarily a new algorithm, the paper should make it clear how
580 to reproduce that algorithm.
 - 581 (b) If the contribution is primarily a new model architecture, the paper should describe
582 the architecture clearly and fully.
 - 583 (c) If the contribution is a new model (e.g., a large language model), then there should
584 either be a way to access this model for reproducing the results or a way to reproduce
585 the model (e.g., with an open-source dataset or instructions for how to construct
586 the dataset).
 - 587 (d) We recognize that reproducibility may be tricky in some cases, in which case
588 authors are welcome to describe the particular way they provide for reproducibility.
589 In the case of closed-source models, it may be that access to the model is limited in
590 some way (e.g., to registered users), but it should be possible for other researchers
591 to have some path to reproducing or verifying the results.

592 **5. Open access to data and code**

593 Question: Does the paper provide open access to the data and code, with sufficient instruc-
594 tions to faithfully reproduce the main experimental results, as described in supplemental
595 material?

596 Answer: [Yes]

597 Justification: Code and data will be released upon acceptance.

598 Guidelines:

- 599 • The answer NA means that paper does not include experiments requiring code.
- 600 • Please see the NeurIPS code and data submission guidelines (<https://nips.cc/public/guides/CodeSubmissionPolicy>) for more details.
- 601 • While we encourage the release of code and data, we understand that this might not be possible, so "No" is an acceptable answer. Papers cannot be rejected simply for not including code, unless this is central to the contribution (e.g., for a new open-source benchmark).
- 602 • The instructions should contain the exact command and environment needed to run to 603 reproduce the results. See the NeurIPS code and data submission guidelines (<https://nips.cc/public/guides/CodeSubmissionPolicy>) for more details.
- 604 • The authors should provide instructions on data access and preparation, including how 605 to access the raw data, preprocessed data, intermediate data, and generated data, etc.
- 606 • The authors should provide scripts to reproduce all experimental results for the new 607 proposed method and baselines. If only a subset of experiments are reproducible, they 608 should state which ones are omitted from the script and why.
- 609 • At submission time, to preserve anonymity, the authors should release anonymized 610 versions (if applicable).
- 611 • Providing as much information as possible in supplemental material (appended to the 612 paper) is recommended, but including URLs to data and code is permitted.
- 613

614 6. Experimental setting/details

615 Question: Does the paper specify all the training and test details (e.g., data splits, hyper-
616 parameters, how they were chosen, type of optimizer, etc.) necessary to understand the
617 results?

618 Answer: [Yes]

619 Justification: We provide thorough implementation details in the paper and supplement.

620 Guidelines:

- 621 • The answer NA means that the paper does not include experiments.
- 622 • The experimental setting should be presented in the core of the paper to a level of detail
623 that is necessary to appreciate the results and make sense of them.
- 624 • The full details can be provided either with the code, in appendix, or as supplemental
625 material.

630 7. Experiment statistical significance

631 Question: Does the paper report error bars suitably and correctly defined or other appropriate
632 information about the statistical significance of the experiments?

633 Answer: [No]

634 Justification: Our evaluation follows the standard deterministic benchmarking setup com-
635 monly used in the protein design literature.

636 Guidelines:

- 637 • The answer NA means that the paper does not include experiments.
- 638 • The authors should answer "Yes" if the results are accompanied by error bars, confi-
639 dence intervals, or statistical significance tests, at least for the experiments that support
640 the main claims of the paper.
- 641 • The factors of variability that the error bars are capturing should be clearly stated (for
642 example, train/test split, initialization, random drawing of some parameter, or overall
643 run with given experimental conditions).
- 644 • The method for calculating the error bars should be explained (closed form formula,
645 call to a library function, bootstrap, etc.)
- 646 • The assumptions made should be given (e.g., Normally distributed errors).

647 • It should be clear whether the error bar is the standard deviation or the standard error
648 of the mean.
649 • It is OK to report 1-sigma error bars, but one should state it. The authors should
650 preferably report a 2-sigma error bar than state that they have a 96% CI, if the hypothesis
651 of Normality of errors is not verified.
652 • For asymmetric distributions, the authors should be careful not to show in tables or
653 figures symmetric error bars that would yield results that are out of range (e.g. negative
654 error rates).
655 • If error bars are reported in tables or plots, The authors should explain in the text how
656 they were calculated and reference the corresponding figures or tables in the text.

657 **8. Experiments compute resources**

658 Question: For each experiment, does the paper provide sufficient information on the com-
659 puter resources (type of compute workers, memory, time of execution) needed to reproduce
660 the experiments?

661 Answer: [\[Yes\]](#)

662 Justification: We detail the compute requirements in the implementation details.

663 Guidelines:

664 • The answer NA means that the paper does not include experiments.
665 • The paper should indicate the type of compute workers CPU or GPU, internal cluster,
666 or cloud provider, including relevant memory and storage.
667 • The paper should provide the amount of compute required for each of the individual
668 experimental runs as well as estimate the total compute.
669 • The paper should disclose whether the full research project required more compute
670 than the experiments reported in the paper (e.g., preliminary or failed experiments that
671 didn't make it into the paper).

672 **9. Code of ethics**

673 Question: Does the research conducted in the paper conform, in every respect, with the
674 NeurIPS Code of Ethics <https://neurips.cc/public/EthicsGuidelines>?

675 Answer: [\[Yes\]](#)

676 Justification: We have reviewed the ethics guidelines and find our paper conforms.

677 Guidelines:

678 • The answer NA means that the authors have not reviewed the NeurIPS Code of Ethics.
679 • If the authors answer No, they should explain the special circumstances that require a
680 deviation from the Code of Ethics.
681 • The authors should make sure to preserve anonymity (e.g., if there is a special consid-
682 eration due to laws or regulations in their jurisdiction).

683 **10. Broader impacts**

684 Question: Does the paper discuss both potential positive societal impacts and negative
685 societal impacts of the work performed?

686 Answer: [\[Yes\]](#)

687 Justification: See conclusion section

688 Guidelines:

689 • The answer NA means that there is no societal impact of the work performed.
690 • If the authors answer NA or No, they should explain why their work has no societal
691 impact or why the paper does not address societal impact.
692 • Examples of negative societal impacts include potential malicious or unintended uses
693 (e.g., disinformation, generating fake profiles, surveillance), fairness considerations
694 (e.g., deployment of technologies that could make decisions that unfairly impact specific
695 groups), privacy considerations, and security considerations.

696 • The conference expects that many papers will be foundational research and not tied
 697 to particular applications, let alone deployments. However, if there is a direct path to
 698 any negative applications, the authors should point it out. For example, it is legitimate
 699 to point out that an improvement in the quality of generative models could be used to
 700 generate deepfakes for disinformation. On the other hand, it is not needed to point out
 701 that a generic algorithm for optimizing neural networks could enable people to train
 702 models that generate Deepfakes faster.
 703 • The authors should consider possible harms that could arise when the technology is
 704 being used as intended and functioning correctly, harms that could arise when the
 705 technology is being used as intended but gives incorrect results, and harms following
 706 from (intentional or unintentional) misuse of the technology.
 707 • If there are negative societal impacts, the authors could also discuss possible mitigation
 708 strategies (e.g., gated release of models, providing defenses in addition to attacks,
 709 mechanisms for monitoring misuse, mechanisms to monitor how a system learns from
 710 feedback over time, improving the efficiency and accessibility of ML).

711 **11. Safeguards**

712 Question: Does the paper describe safeguards that have been put in place for responsible
 713 release of data or models that have a high risk for misuse (e.g., pretrained language models,
 714 image generators, or scraped datasets)?

715 Answer: [NA]

716 Justification: Paper poses no such risks.

717 Guidelines:

718 • The answer NA means that the paper poses no such risks.
 719 • Released models that have a high risk for misuse or dual-use should be released with
 720 necessary safeguards to allow for controlled use of the model, for example by requiring
 721 that users adhere to usage guidelines or restrictions to access the model or implementing
 722 safety filters.
 723 • Datasets that have been scraped from the Internet could pose safety risks. The authors
 724 should describe how they avoided releasing unsafe images.
 725 • We recognize that providing effective safeguards is challenging, and many papers do
 726 not require this, but we encourage authors to take this into account and make a best
 727 faith effort.

728 **12. Licenses for existing assets**

729 Question: Are the creators or original owners of assets (e.g., code, data, models), used in
 730 the paper, properly credited and are the license and terms of use explicitly mentioned and
 731 properly respected?

732 Answer: [Yes]

733 Justification: All existing models and datasets are properly credited.

734 Guidelines:

735 • The answer NA means that the paper does not use existing assets.
 736 • The authors should cite the original paper that produced the code package or dataset.
 737 • The authors should state which version of the asset is used and, if possible, include a
 738 URL.
 739 • The name of the license (e.g., CC-BY 4.0) should be included for each asset.
 740 • For scraped data from a particular source (e.g., website), the copyright and terms of
 741 service of that source should be provided.
 742 • If assets are released, the license, copyright information, and terms of use in the
 743 package should be provided. For popular datasets, paperswithcode.com/datasets
 744 has curated licenses for some datasets. Their licensing guide can help determine the
 745 license of a dataset.
 746 • For existing datasets that are re-packaged, both the original license and the license of
 747 the derived asset (if it has changed) should be provided.

748 • If this information is not available online, the authors are encouraged to reach out to
749 the asset's creators.

750 **13. New assets**

751 Question: Are new assets introduced in the paper well documented and is the documentation
752 provided alongside the assets?

753 Answer: **[Yes]**

754 Justification: New datasets, code, and models will be released upon publication.

755 Guidelines:

756 • The answer NA means that the paper does not release new assets.

757 • Researchers should communicate the details of the dataset/code/model as part of their
758 submissions via structured templates. This includes details about training, license,
759 limitations, etc.

760 • The paper should discuss whether and how consent was obtained from people whose
761 asset is used.

762 • At submission time, remember to anonymize your assets (if applicable). You can either
763 create an anonymized URL or include an anonymized zip file.

764 **14. Crowdsourcing and research with human subjects**

765 Question: For crowdsourcing experiments and research with human subjects, does the paper
766 include the full text of instructions given to participants and screenshots, if applicable, as
767 well as details about compensation (if any)?

768 Answer: **[NA]**

769 Justification: No human subjects.

770 Guidelines:

771 • The answer NA means that the paper does not involve crowdsourcing nor research with
772 human subjects.

773 • Including this information in the supplemental material is fine, but if the main contribu-
774 tion of the paper involves human subjects, then as much detail as possible should be
775 included in the main paper.

776 • According to the NeurIPS Code of Ethics, workers involved in data collection, curation,
777 or other labor should be paid at least the minimum wage in the country of the data
778 collector.

779 **15. Institutional review board (IRB) approvals or equivalent for research with human
780 subjects**

781 Question: Does the paper describe potential risks incurred by study participants, whether
782 such risks were disclosed to the subjects, and whether Institutional Review Board (IRB)
783 approvals (or an equivalent approval/review based on the requirements of your country or
784 institution) were obtained?

785 Answer: **[NA]**

786 Justification: No human subjects.

787 Guidelines:

788 • The answer NA means that the paper does not involve crowdsourcing nor research with
789 human subjects.

790 • Depending on the country in which research is conducted, IRB approval (or equivalent)
791 may be required for any human subjects research. If you obtained IRB approval, you
792 should clearly state this in the paper.

793 • We recognize that the procedures for this may vary significantly between institutions
794 and locations, and we expect authors to adhere to the NeurIPS Code of Ethics and the
795 guidelines for their institution.

796 • For initial submissions, do not include any information that would break anonymity (if
797 applicable), such as the institution conducting the review.

798 **16. Declaration of LLM usage**

799 Question: Does the paper describe the usage of LLMs if it is an important, original, or
800 non-standard component of the core methods in this research? Note that if the LLM is used
801 only for writing, editing, or formatting purposes and does not impact the core methodology,
802 scientific rigorosity, or originality of the research, declaration is not required.

803 Answer: [NA]

804 Justification: LLM are not part of the core method.

805 Guidelines:

806 • The answer NA means that the core method development in this research does not
807 involve LLMs as any important, original, or non-standard components.

808 • Please refer to our LLM policy (<https://neurips.cc/Conferences/2025/LLM>)
809 for what should or should not be described.



Ambient Proteins

Training Diffusion Models on Noisy Structures

Supplement

Anonymous Author(s)

Affiliation
Address
email

1 A Evaluation Metrics

2 Evaluation of a protein generative model is challenging and there have been a few metrics that have
3 been proposed. In what follows, we explain standard metrics in the protein-generative modeling
4 literature that we will use in our Experimental Results section. Our experiments report using Proteína's
5 definitions of the metrics when possible.

6 **Designability** (also referred to as refoldability) assesses the structural plausibility of generated
7 proteins. Given a generated backbone, ProteinMPNN [1] generates eight plausible amino acid
8 sequences for that backbone. ESMFold then folds each sequence and the resulting eight structures
9 are compared to the original backbone. The self-consistency RMSD (scRMSD) is defined as the
10 smallest root mean squared deviation between the generated backbone and each of the eight refolded
11 structures. A backbone is considered *designable* if $\text{scRMSD} < 2 \text{ \AA}$ and designability is defined as
12 the percentage of generated backbones that meet this criterion.

Diversity quantifies the structural variability among the generated proteins. Designable backbones
are clustered using Foldseek with a TM-score threshold of 0.5. Diversity is then defined as:

$$\text{Diversity} = \frac{\text{Number of Designable Clusters}}{\text{Number of Designable Samples}}.$$

13 This metric reflects the proportion of structurally distinct (i.e., non-redundant) designable backbones
14 among all designable samples.

15 B Secondary Structure conditioning

16 Previous work [2] has explored conditioning protein structure generation on CATH labels, a form of
17 hierarchical classification derived from the orientation and spatial organization of protein secondary
18 structures [5]. In this setting, every residue in a protein sequence is typically assigned the same CATH
19 label. In contrast, we propose a more fine-grained approach. Rather than relying on the manually
20 curated and coarse-grained CATH classification, we condition our model directly on secondary
21 structure annotations at the residue level. Each residue is assigned a label corresponding to its local
22 secondary structure (e.g., helix, strand, coil), allowing the model to leverage localized structural
23 context during generation.

24 We train a variant of our model with partial conditioning, in which the model is conditioned on
25 the secondary structure sequence, without introducing any additional modifications to the input or
26 architecture. We show designable samples conditioned on the secondary structure extracted from real

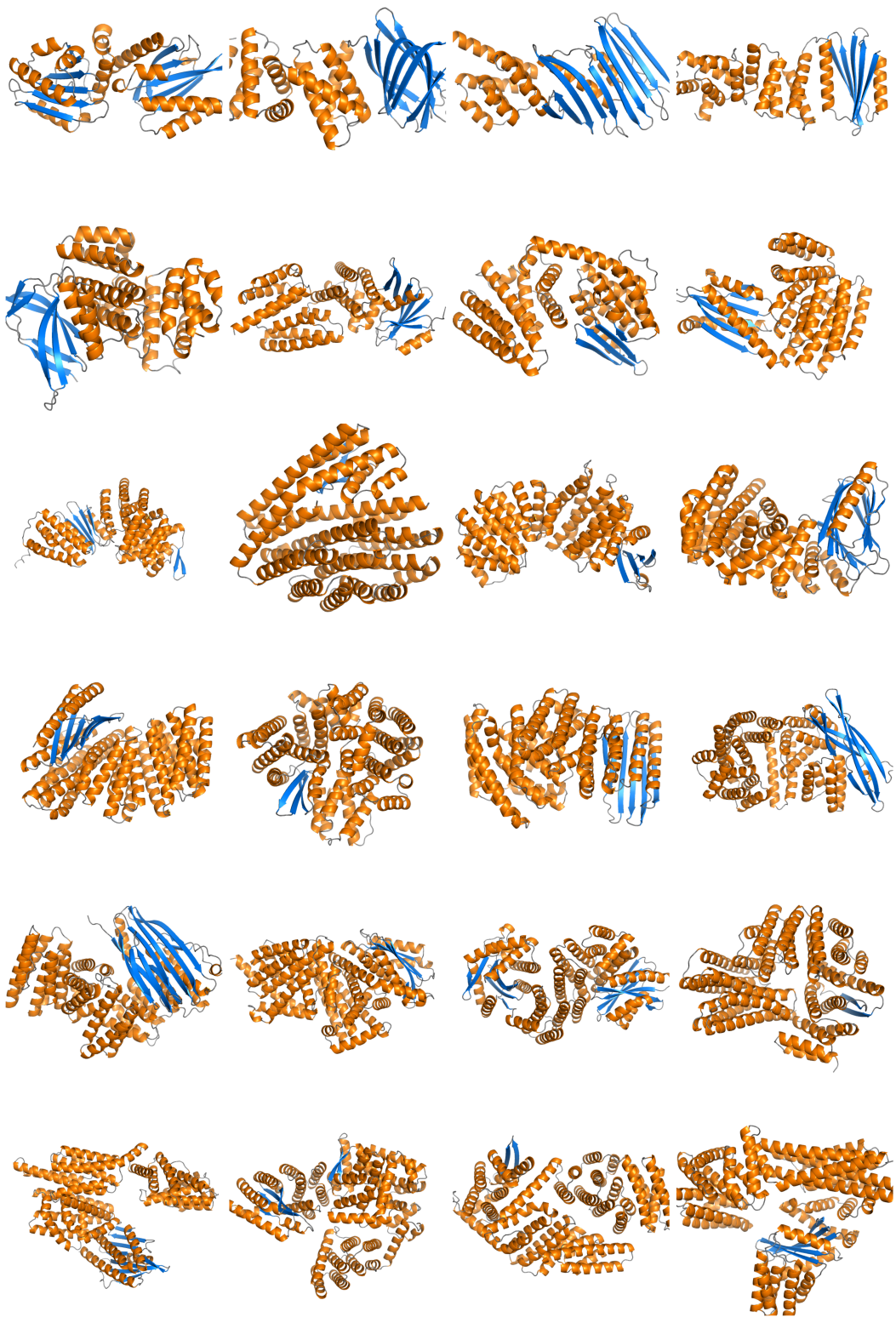


Figure 1: **Qualitative visualizations of unconditional generations.** Our model is capable of producing diverse, multi-domain long proteins.

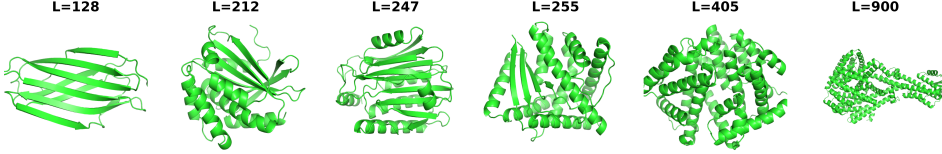


Figure 2: **Secondary Structure Conditioned Samples.** We generate proteins using a model variant trained with secondary structure conditioning. To guide generation, we extract secondary structure strings from existing proteins and use this coarse-grained structural representation as input. This conditioning enables the model to produce diverse and designable protein structures.

27 proteins in Figure 2. These results demonstrate that, even with coarse-grained secondary structure
 28 conditioning, our model can generate long, diverse proteins exhibiting a wide range of folds.

29 C Model and Training Hyperparameters

30 Table I includes a more thorough list of the hyperparameters used for our experiments.

31 D Full Motif Scaffolding Results

32 Table 2 and table 3 represent the numbers of unique successful scaffolds generated by Genie2 [3],
 33 RFDiffusion [6], Proteína [2] and *Ambient Protein Diffusion* for each motif in the benchmark dataset
 34 in Genie2.

35 E Full Training Algorithm and Implementation Details

36 E.1 Additional Implementation Details

37 **Loss buffer.** The loss rescaling introduced in the main paper ensures balanced weighting across
 38 noise levels. At the same time, it also introduces a potential instability: the loss explodes as $\sigma(t)$
 39 approaches $\sigma(t_i)$. To mitigate this instability, we define a buffer zone around each protein’s assigned
 40 noise level. Specifically, given a protein’s assigned noise level t_i , it is only used during training at
 41 timesteps $t + \tau$, where τ is a buffer hyperparameter that controls the exclusion margin. This constraint
 42 prevents the model from encountering degenerate gradient behavior near the rescaling boundaries
 43 and is only applied to medium and low confidence structures ($\text{pLDDT} < 90$). We underline that is
 44 similar to how in normal diffusion there is a buffer time zone around $t = 0$ that is never sampled.

45 **Ambient in high-noise regime.** As explained in the main paper, each protein is only used for a subset
 46 of diffusion times according to its average pLDDT value. The proteins that have super high PLDDT
 47 (> 90) are considered clean data and can be used with the normal training objective. However, as
 48 found in [4], using the Ambient training objective for high-noise might be useful even if clean data is
 49 available. Intuitively, this objective prevents memorization and promotes diversity in the outputs. We
 50 ablated this design choice, and we found a slight increase in diversity for the same designability by
 51 using this. Hence, we used this tool from [4] for all our Ambient Protein Diffusion trainings.

52 E.2 Algorithm

53 We provide the full algorithm in Algorithm I. We commit to open-sourcing our code and models to
 54 facilitate the broader adoption of our method from the community.

Hyperparameter	Genie2	Ambient (Stage 1)	Stage 2	Stage 3
<i>Diffusion</i>				
Number of timesteps	1,000	-	-	-
Noise schedule	Cosine	-	-	-
Ambient walls	-	(600,900)	(600,900)	(600,900)
<i>Model Architecture</i>				
Single feature dimension	384	-	-	-
Pair feature dimension	128	-	-	-
Pair transform layers	5	8	8	8
Triangle dropout	0.25	-	-	-
Structure layers	8	-	-	-
<i>Training</i>				
Optimizer	AdamW	-	-	-
Number of training proteins	586k	196k	269k	291k
Number epochs	40	200	50	20
Warmup iterations	10,000	1,000	500	100
Total batch size	384	384	96	48
Learning rate	1.0×10^{-4}	1.0×10^{-4}	1.0×10^{-5}	1.0×10^{-5}
Weight decay	0.05	-	-	-
Minimum protein length	20	20	50	50
Maximum protein length	256	256	512	768
Minimum mean pLDDT	80	70	70	70
<i>Compute Resources</i>				
Number of GPUs	48	48	48	48
Training time	18 hr	18hr	48hr	48hr

Table 1: **Hyperparameters of the diffusion protein model.** Dashes (-) indicate that the value is the same as the previous column. The Ambient walls correspond to the assigned diffusion times based on the protein’s pLDDT (times are from 1 to 1000). Proteins with pLDDT > 90 are used everywhere. Proteins with pLDDT > 80 are used for times in [600, 1000] and proteins with pLDDT > 70 are used for times in [900, 1000]. We underline that these hyperparameters were not particularly optimized, and even more benefits might be observed by properly tuning these values.

Motif Name	Genie 2	RFDiffusion	Proteína	<i>Ambient Protein Diffusion</i>
6E6R_long	415	381	713	601
6EXZ_long	326	167	290	432
6E6R_med	272	151	417	406
1YCR	134	7	249	146
5TRV_long	97	23	179	119
6EXZ_med	54	25	43	69
7MRX_128	27	66	51	44
6E6R_short	26	23	56	27
5TRV_med	23	10	22	23
7MRX_85	23	13	31	17
3IXT	14	3	8	4
5TPN	8	5	4	11
7MRX_60	5	1	2	1
1QJG	5	1	3	5
5TRV_short	3	1	1	3
5YUI	3	1	5	4
4ZYP	3	6	11	3
6EXZ_short	2	1	3	3
1PRW	1	1	1	1
5IUS	1	1	1	1
1BCF	1	1	1	1
5WN9	1	0	2	1
2KL8	1	1	1	1
4JHW	0	0	0	0
Total	1445	889	2094	1923

Table 2: **Detailed single motif scaffolding results.** Ambient Protein Diffusion achieves superior results to Genie 2 and RFDiffusion and performs on par with Proteina. Crucially, our model achieves these results zero-shot, i.e., unlike Proteina, it is not optimized for motif scaffolding and still achieves comparable performance while being an order of magnitude smaller.

Motif Name	Genie 2	<i>Ambient Protein Diffusion</i>
3BIK+3BP5	17	23
1PRW_four	11	38
1PRW_two	8	15
4JHW+5WN9	4	12
2B5I	0	1
3NTN	0	0
Total	40	89

Table 3: **Multi-motif scaffolding results.** Ambient Protein Diffusion achieves consistently superior results to the predecessor Genie-2 model, despite using the same architecture, i.e. the benefit comes from better use of the data. The motif 2B5I is only solved by Ambient Protein Diffusion.

Algorithm 1 Ambient Protein Diffusion: Training Algorithm.

Require: untrained network h_θ , dataset $\mathcal{D} = \{(x_0^{(i)}, \text{pLDDT}^{(i)})\}_{i=1}^N$, pLDDT to diffusion time mapping function $f : [0, 100] \mapsto \mathbb{R}^+$, noise scheduling $\sigma(t)$, batch size B , diffusion time T , buffer τ .

- 1: $\tilde{\mathcal{D}} \leftarrow \left\{ \left(x_0^{(i)} + f(\text{pLDDT}^{(i)})\epsilon^{(i)}, f(\text{pLDDT}^{(i)}) \right) \mid (x_0^{(i)}, \text{pLDDT}^{(i)}) \in \mathcal{D}, \epsilon^{(i)} \sim \mathcal{N}(0, I_d) \right\}$ \triangleright Noise each point in the training set according to its pLDDT and get (noisy, noise level) pairs.
- 2: **while** not converged **do**
- 3: $t_s^{(1)}, \dots, t_s^{(B)} \leftarrow$ Sample uniformly B times in $[0, T]$ \triangleright Sample diffusion times for this batch.
- 4: $\tilde{\mathcal{D}}_p \leftarrow \text{shuffle}(\tilde{\mathcal{D}})$ \triangleright Shuffle dataset.
- 5: $\text{loss} \leftarrow 0$ \triangleright Initialize loss.
- 6: $\text{pos} \leftarrow 0$ \triangleright Initialize index at shuffled dataset.
- 7: **for** $i \in [1, B]$ **do**
- 8: **while** True **do** \triangleright find the first eligible point
- 9: $y, t_y \leftarrow \tilde{\mathcal{D}}_p[\text{pos}]$
- 10: **if** $t_y \geq t_s^i + \tau$ **then**
- 11: **break**
- 12: **else**
- 13: $\text{pos} \leftarrow \text{pos} + 1$ \triangleright Move to the next point in the dataset.
- 14: **end if**
- 15: **end while**
- 16: $\epsilon \sim \mathcal{N}(0, I)$ \triangleright Sample noise.
- 17: $t \leftarrow t_s^{(i)}$ \triangleright Time to be used in this training update.
- 18: $t_i \leftarrow t_y$ \triangleright Assigned time based on the PLDDT value
- 19: $x_{t_i} \leftarrow y$ \triangleright Noised point to the assigned time.
- 20: $x_t \leftarrow x_{t_i} + \sqrt{\sigma^2(t) - \sigma^2(t_i)}\epsilon$ \triangleright Add additional noise.
- 21: $\alpha(t, t_i) \leftarrow \frac{\sigma^2(t) - \sigma^2(t_i)}{\sigma^2(t)}$.
- 22: $w(t, t_i) \leftarrow \frac{\sigma^4(t)}{(\sigma^2(t) - \sigma^2(t_i))^2}$. \triangleright Loss reweighting.
- 23: $\text{loss} \leftarrow \text{loss} + w(t, t_i) \|\alpha(t, t_i)h_\theta(x_t, t) + (1 - \alpha(t, t_i))x_t - x_{t_i}\|^2$ \triangleright Ambient loss
- 24: **end for**
- 25: $\text{loss} \leftarrow \frac{\text{loss}}{B}$ \triangleright Compute average loss.
- 26: $\theta \leftarrow \theta - \eta \nabla_\theta \text{loss}$ \triangleright Update network parameters via backpropagation.
- 27: **end while**

55 **References**

56 [1] Justas Dauparas, Ivan Anishchenko, Nathaniel Bennett, Hua Bai, Robert J Ragotte, Lukas F
57 Milles, Basile IM Wicky, Alexis Courbet, Rob J de Haas, Neville Bethel, et al. Robust deep
58 learning-based protein sequence design using proteinmpnn. *Science*, 378(6615):49–56, 2022.

59 [2] Tomas Geffner, Kieran Didi, Zuobai Zhang, Danny Reidenbach, Zhonglin Cao, Jason Yim, Mario
60 Geiger, Christian Dallago, Emine Kucukbenli, Arash Vahdat, et al. Proteina: Scaling flow-based
61 protein structure generative models. *arXiv preprint arXiv:2503.00710*, 2025.

62 [3] Yeqing Lin, Minji Lee, Zhao Zhang, and Mohammed AlQuraishi. Out of many, one: Designing
63 and scaffolding proteins at the scale of the structural universe with genie 2. *arXiv preprint*
64 *arXiv:2405.15489*, 2024.

65 [4] Kulin Shah, Alkis Kalavasis, Adam R. Klivans, and Giannis Daras. Does generation require
66 memorization? creative diffusion models using ambient diffusion, 2025.

67 [5] Ian Sillitoe, Nicola Bordin, Natalie Dawson, Vaishali P Waman, Paul Ashford, Harry M Scholes,
68 Camilla SM Pang, Laurel Woodridge, Clemens Rauer, Neeladri Sen, et al. Cath: increased
69 structural coverage of functional space. *Nucleic acids research*, 49(D1):D266–D273, 2021.

70 [6] Joseph L Watson, David Juergens, Nathaniel R Bennett, Brian L Trippe, Jason Yim, Helen E
71 Eisenach, Woody Ahern, Andrew J Borst, Robert J Ragotte, Lukas F Milles, et al. De novo
72 design of protein structure and function with rfdiffusion. *Nature*, 620(7976):1089–1100, 2023.